



CLINICAL RESEARCH ARTICLE

B-cell-specific accumulation of inclusion bodies loaded with HLA class II molecules in patients with mucopolidosis II (I-cell disease)

Ayano Yokoi¹, Yo Niida², Mondo Kuroda¹, Yoko Imi-Hashida¹, Tomoko Toma¹ and Akihiro Yachie¹

BACKGROUND: I-cell disease is characterized by the presence of vacuole-like inclusions in lymphocytes. However, the nature and clinical significance of these inclusions have seldom been characterized. In this study, the authors tried to elucidate the distribution in different lymphocyte subpopulations, and the histological nature of the inclusions.

METHODS: Blood samples from three unrelated patients were analyzed. Lymphocyte subpopulations were separated using monoclonal antibodies conjugated to immunomagnetic beads. Cytochemical studies were performed using FITC-conjugated lectins. The expressions of surface and cytoplasmic class II molecules were analyzed by flow cytometry.

RESULTS: Virtually all B cells from the patients contained the inclusions. In contrast, CD4⁺ T cells, CD8⁺ T cells, natural killer cells, monocytes, or neutrophils did not contain the inclusions. Both fibroblasts and B cells from I-cell patients were stained intensely by multiple FITC-conjugated lectins with distinct binding profiles. The inclusions of B cells were stained intensely by fluorescence-conjugated antibodies against class II antigens.

CONCLUSIONS: Inclusions in I-cell disease reflect the accumulation of HLA class II molecules within B cells. These results suggest a potential role for *N*-acetylglucosamine-1-phosphotransferase in immune functions. Furthermore, the fact that only B cells contain the inclusions provides a novel diagnostic aid for the diagnosis of I-cell disease.

Pediatric Research (2019) 86:85–91; <https://doi.org/10.1038/s41390-018-0234-2>

Mucopolidosis type II (MLII; MIM#252500) was first reported in 1967 by Leroy and DeMars;¹ it was characterized by developmental delays, coarse features, thoracic deformity, subluxation of hip joints, short stature, joint contracture, thick skin, and gingival hypertrophy.^{2,3} The estimated incidence is 1 in 25,000 among the Japanese.⁴ It is caused by a mutation of *GNPTAB* located at 4q23.2.^{5,6} Mutations of this particular gene result in defects of the α and β subunits of *N*-acetylglucosamine (GlcNac)-1-phosphotransferase, which is an enzyme localized within the Golgi membrane; it is composed of six subunits, including two α subunits, two β -subunits, and two γ -subunits. GlcNac-1-phosphotransferase acts at the first step of mannose 6-phosphate (M6P) addition to lysosomal enzymes.⁷ Once M6P is successfully added, the lysosomal enzymes are recognized by M6P receptors on the Golgi membrane and are transferred to lysosomes.⁸ A lack of GlcNac-1-phosphotransferase results in the failure of lysosomal enzyme transport to lysosomes.⁹ Consequently, undigested junk materials accumulate within the lysosomes.

MLII is also called inclusion-cell (I-cell) disease, because the fibroblasts derived from patients contain abundant inclusions within the cytoplasm. These inclusions are observed not only in cultured skin fibroblasts, but also in a variety of other cell types *in vivo*, including peripheral blood lymphocytes.^{10–12} For this reason, the detection of lymphocytes with inclusions, or vacuoles, may serve as an aid for diagnosing this rare disease, in addition to

the determination of serum activity of lysosomal enzymes overflowing from the cells. However, only a fraction of lymphocytes contain the characteristic vacuole-like inclusions.¹³ To date, the exact nature of the inclusions within the lymphocytes remains unknown. Similarly, it remains unknown why only a fraction of the lymphocytes in patients with I-cell disease have the vacuole-like inclusions.

In this study, we compared the histochemical nature of the inclusions in fibroblasts and lymphocytes using a lectin-binding assay. In addition, we tried to identify particular lymphocyte subpopulations that might specifically and exclusively contain the inclusions.

METHODS

Patients

We evaluated three unrelated Japanese patients with no parental consanguinity. All patients showed typical clinical features of MLII, such as a coarse face, psychomotor delay, hypotonia, gingival hypertrophy, thick skin, and restricted joint movement, and had distinct mutations in the *GNPTAB* gene.

Case 1 was a 12-year-old girl. A coarse face, hypotonia, and difficult feeding were noted immediately after birth. She showed growth delays and developmental retardation, and had hepatosplenomegaly, defective osteogenesis, joint contracture, gingiva hypertrophy, and repeated episodes of respiratory tract infection

¹Department of Pediatrics, School of Medicine, Graduate School of Medical Sciences, Kanazawa University, Kanazawa, Japan and ²Division of Clinical Genetics, Multidisciplinary Medical Center, Kanazawa Medical University Hospital, Uchinada, Japan
Correspondence: Akihiro Yachie (yachie@staff.kanazawa-u.ac.jp)

Received: 7 June 2018 Accepted: 24 October 2018

Published online: 21 November 2018

as she grew older. Lymphocyte inclusions were identified in the peripheral blood. MLII was diagnosed at the age of 2 years based on the high serum levels of lysosomal enzymes and the low levels of enzyme activity within the cultured skin fibroblasts. The diagnosis was confirmed by *GNPTAB* gene mutation analysis.

Case 2 was a boy referred to our hospital at the age of 2 months due to a coarse face and bone fractures. Joint contractures, gingival hypertrophy, and the identification of lymphocyte inclusions prompted the diagnosis of MLII by the detection of high serum levels of lysosomal enzyme activity. *GNPTAB* gene analysis confirmed the diagnosis. The patient experienced repeated episodes of bronchiolitis and died at the age of 6 years and 1 month due to pulmonary hypertension.

Case 3 was a 4-year-old boy. Short leg length was noted for both legs in utero by ultrasonographic examination. He was born at 36 weeks of gestation with a birth weight of 1924 g. He was referred to us on the 21st day after birth due to a characteristic facial countenance and bone deformity. Lymphocyte inclusions were noted. He had mutations within the *GNPTAB* gene and the diagnosis of MLII was confirmed. He later developed a coarse face and showed growth delays, psychomotor retardation, impaired bone growth, and joint contractures. He has experienced repeated episodes of airway infection.

Culture of skin fibroblasts

Skin tissues were obtained from the patients with I-cell disease and normal control subjects by means of skin biopsy; these tissues were used for morphological analysis and the establishment of cultured fibroblasts.¹⁴ Informed consent was obtained from the corresponding families. This study involving cultured fibroblasts was approved by the Ethical Committee of Kanazawa University. The established skin fibroblasts were cultured in Ham's F-10 medium supplemented with 10% fetal calf serum and antibiotics at 37 °C under a 5% CO₂-95% air mixture.

Isolation of mononuclear cells and separation of lymphocyte subpopulations

Lymphocytes were prepared from peripheral blood mononuclear cells (PBMCs) by depleting monocytes using anti-CD14 monoclonal antibody (mAb)-coated magnetic beads (Becton Dickinson, San Diego, CA).¹⁵ CD4⁺ T cells, CD8⁺ T cells, CD19⁺ B cells, and CD56⁺ natural killer (NK) cells were purified by positive selection from the lymphocytes using the respective mAb-coated magnetic beads (Becton Dickinson). The purity of each cell population was greater than 95%. Cytospin preparations were made for each cell population for morphological examination and immunohistochemical analysis.

Cytochemical analysis

Cytochemical analysis of skin fibroblasts and B cells was done as described previously using fluorescein isothiocyanate (FITC)-conjugated lectins.¹⁴ Briefly, skin fibroblasts from the patients with I-cell disease and controls were cultured on Lab-Tek chamber slides (Nunc, Naperville, IL) for 3 days. PBMCs were isolated by Ficoll-Hypaque gradient centrifugation. Both the fibroblast preparations and cytospin preparations of PBMCs were washed with phosphate-buffered saline (PBS) and fixed with 4% paraformaldehyde in PBS (pH 7.4) for 10 min at room temperature, then washed with PBS, and blocked with 1% bovine serum albumin (BSA) in PBS for 30 min as described previously. A FITC-conjugated plant lectin library (J-OIL MILLS, Osaka, Japan) was diluted in PBS and used to detect specific sugar chains. Lectins that were in the library and used for the immunostaining analysis included *Agaricus bisporus* agglutinin (ABA; binding specificity, Gal β 1-3GalNAc) and lectins from *Datura stramonium* (DSA; binding specificity, β -D-GlcNAc), *Maackia amurensis* (MAM; binding specificity, α 2-3 Gal β 1-4GlcNAc), *Phaseolus vulgaris* (PHA-L4; binding specificity, GalNAc), *Lotus tetragonolobus* (Lotus; binding specificity, LewisY),

Glycine max (SBA; binding specificity, α GalNAc), and *Sambucus sieboldiana* (SSA; binding specificity, sialic acid α 2-6 Gal/GalNAc). The cells were incubated with FITC-conjugated lectins for 1 h at room temperature. The slides were counterstained with the appropriate dilutions of 4',6-diamidino-2-phenylindole (DAPI) for nuclear staining. The cells were washed with 1% BSA-PBS. After washing with PBS, the slides were embedded in PermaFluor Aqueous Mounting Medium (Thermo Electron Corporation, Waltham, MA) and mounted with coverglasses. The stained cells were examined under a fluorescence microscope.

Cytospin preparations of CD19⁺ B cells from the controls and patients were similarly stained with FITC-conjugated lectins and the lectin-binding profiles were examined as described above.

Immunohistochemistry

Cytospin preparations of CD19⁺ B cells were fixed in cold acetone for 5 min, air-dried, and washed in PBS before staining. FITC-conjugated mAbs against HLA-DR, HLA-DQ, and CLIP, and a phycoerythrin (PE)-conjugated mAb against HLA-DM (Becton Dickinson) were used to stain class II-related molecules in the B-cell preparations.

Flow cytometry

The surface and cytoplasmic expressions of HLA-DR in different lymphocyte subpopulations were compared as follows. PBMCs were stained for cell-surface antigens before cell membrane permeabilization using FITC-conjugated anti-CD4, anti-CD8, anti-CD20, or anti-CD56 mAb (Becton Dickinson). After washing, the cells were fixed and permeabilized with a Cytofix/Cytoperm Plus kit (Becton Dickinson) and then incubated with PE-conjugated anti-HLA-DR at 4 °C for 20 min. Stained cells were analyzed with a FACSCalibur flow cytometer using CellQuest software (BD Bioscience, Tokyo, Japan). After gating FITC-positive cell clusters for each lymphocyte subpopulation, the HLA-DR expression profiles were compared between the surface and cytoplasmic expressions.

The expression of HLA class II molecules was examined in a similar manner. For HLA-DR, HLA-DQ, and CLIP expressions, FITC-conjugated antibodies were used together with PE-conjugated anti-CD19 (Becton Dickinson). For HLA-DM, PE-conjugated antibody was used together with FITC-conjugated anti-CD19 (Becton Dickinson). The mean fluorescence intensity (MFI) of each sample was determined by flow cytometry after gating CD19⁺ B cells. The differences between the surface and cytoplasmic staining intensities were calculated and the data are presented as the Δ MFI.

RESULTS

Morphology of lymphocytes and cultured fibroblasts

Peripheral blood smears from the controls and patients were stained with May-Grünwald solution and the morphology of the lymphocytes was compared (Fig. 1). In control smears, virtually no lymphocyte contained vacuole-like inclusions (Fig. 1a) and only a small number of vacuoles could be detected in monocytes. In contrast, up to 10% of the patient lymphocytes contained many vacuole-like inclusions (Fig. 1b). Occasionally, clusters of extracellular inclusions were observed within the smears from the patients (Fig. 1c). Phase-contrast microscopy images of the cultured skin fibroblasts are shown in Fig. 1d and e. As compared with the control fibroblasts (Fig. 1d), the cultured skin fibroblasts from patients contained a large number of fine vacuoles within the cytoplasm (Fig. 1e). The vacuole-like inclusions in lymphocytes were large in size and had evident inclusions, while those in skin fibroblasts were fine and densely filled the cytoplasm of the fibroblasts.

Vacuole-like inclusions in lymphocyte subpopulations

We first examined the morphological nature of the vacuole-like inclusions in the peripheral blood smears from the I-cell disease

patients. As described previously, a fraction of the lymphocytes contained abundant vacuole-like inclusions within the cytoplasm (Fig. 2). It was intriguing that although the majority of the lymphocytes contained only a few, if any, vacuole-like inclusions, there was a small fraction of lymphocytes with abundant vacuole-like inclusions within the cytoplasm, indicating a clear distinction between the vacuole-negative cells (Fig. 2a–j) and vacuole-positive cells (Fig. 2k–o). To determine whether the vacuole-like inclusions were restricted to certain cell subpopulations, lymphocyte subpopulations were isolated and their morphologies were compared after staining with May–Grünwald solution. In all three patients, the CD19⁺ B cells contained significant numbers of vacuole-like inclusions. In marked contrast, the vacuole-like inclusions were never detected in other cell types, including CD4⁺ T cells, CD8⁺ T cells, and CD56⁺ NK cells (Fig. 3). The mean

percentages (\pm standard deviation (SD)) of cells with vacuole-like inclusions among the total leukocytes, mononuclear cells, lymphocytes, and B lymphocytes were $9.5\% \pm 2.0\%$, $17.0\% \pm 2.1\%$, $22.0\% \pm 4.6\%$, and $98.1\% \pm 0.4\%$, respectively (Table 1).

Lectin-binding profiles of lymphocytes and cultured fibroblasts
It was suggested from the above observations that different mechanisms of cytoplasmic vacuole formation exist for different

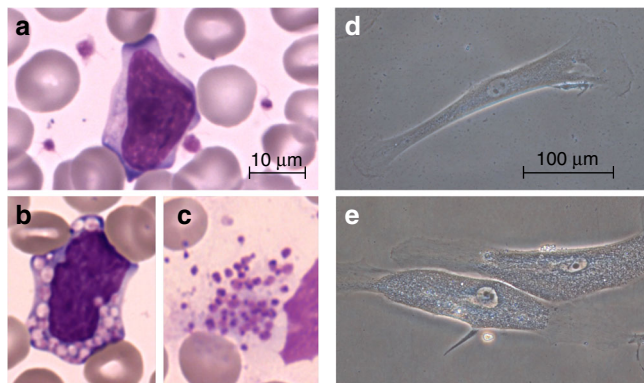


Fig. 1 Morphological comparison of lymphocytes and skin fibroblasts. The morphology of lymphocytes and skin fibroblasts from the control and I-cell disease patients were compared. Although the circulating lymphocytes from the normal controls contained only a few or no vacuoles (a), a fraction of lymphocytes from I-cell patients contained many vacuole-like inclusions within the cytoplasm (b). Occasionally, clusters of granular materials were found in the blood smears (c). Skin fibroblasts from the controls did not show any vacuoles within the cytoplasm (d), whereas those from I-cell disease patients showed a cytoplasm packed with many fine vesicles (e)

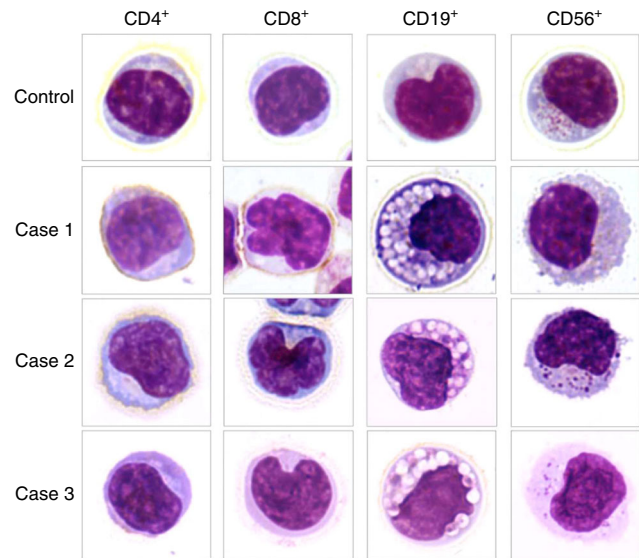


Fig. 3 Distinct morphologies of different lymphocyte lineages. Peripheral blood lymphocytes were separated into different subpopulations and their morphologies were compared after staining of the cytospin preparations. None of the separated lymphocyte subpopulations, including CD4⁺ T cells, CD8⁺ T cells, CD19⁺ B cells, and CD56⁺ NK cells, from the normal controls contained cytoplasmic vacuoles (upper row). Although the CD4⁺ T cells, CD8⁺ T cells, and CD56⁺ NK cells from the I-cell disease patients did not contain vacuole-like inclusions, the CD19⁺ B cells contained a large amount of vacuole-like inclusions (lower rows)

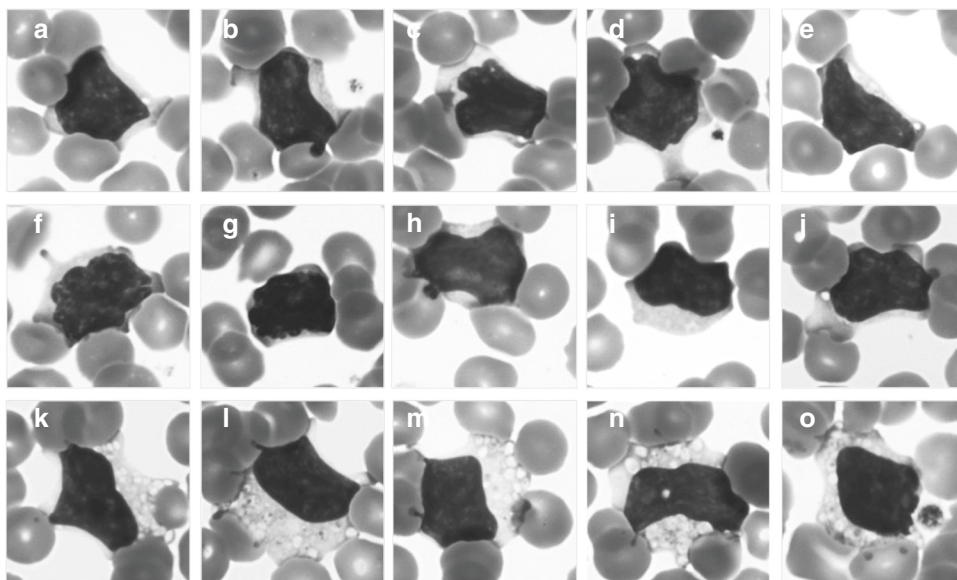


Fig. 2 Peripheral blood lymphocytes of I-cell disease patients. Many of the peripheral blood lymphocytes from I-cell disease patients contained only a few, if any, vacuoles within the cytoplasm (a–j). In contrast, a small fraction of lymphocytes contained many vacuole-like inclusions (k–o)

Cases	Leukocytes	Neutrophils	Mononuclear cells	Monocytes	Lymphocytes	B cells	Non-B cells
Case 1	8.3%	<0.1%	14.0%	<0.1%	17.3%	98.6%	<0.1%
Case 2	8.6%	<0.1%	18.3%	<0.1%	20.3%	97.8%	<0.1%
Case 3	13.0%	<0.1%	18.6%	<0.1%	28.3%	97.8%	<0.1%
Mean (±SD)	9.5 ± 2.0%	<0.1%	17.0 ± 2.1%	<0.1%	22.0 ± 4.6 %	98.1 ± 0.4%	<0.1%

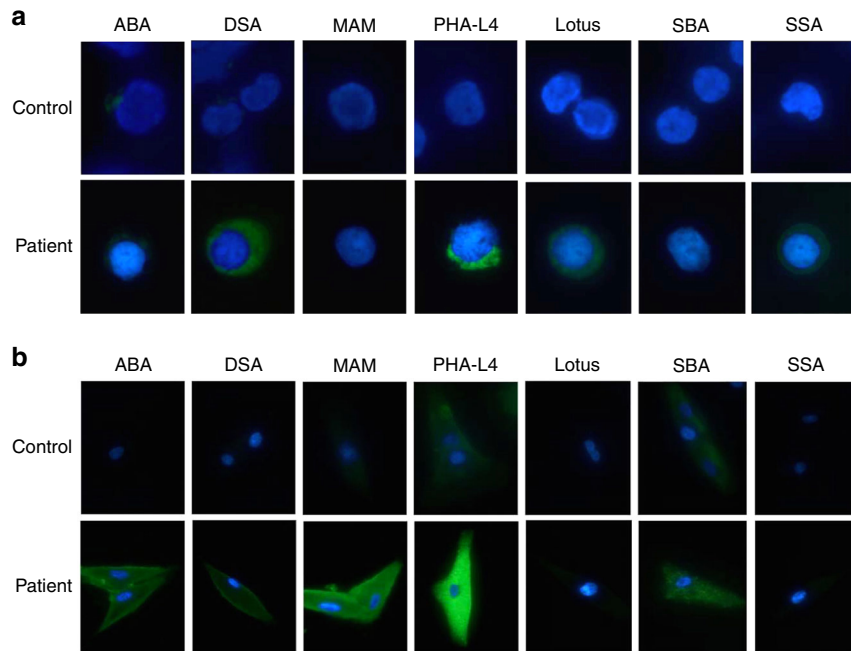


Fig. 4 Lectin-binding profiles of B lymphocytes and skin fibroblasts. The peripheral blood B cells (a) and skin fibroblasts (b) of the controls and patients were stained with FITC-conjugated lectins. The nuclei were stained with DAPI

types of cells. Consequently, fibroblasts and lymphocytes may have different types of inclusions. As such, we next examined whether these two cell populations showed distinct cytochemical characteristics using FITC-conjugated lectin-binding analysis. The lectin-binding profiles of B cells and cultured skin fibroblasts are shown in Fig. 4. Little lectin binding was observed within the control B cells. In contrast, strong binding of PHA and weak, but significant, binding of DSA and Lotus were seen in the patient B cells (Fig. 4a). Only a low level of PHA and SBA binding was observed in the control fibroblasts. In contrast, intense binding of PHA and significant levels of binding of ABA, DSA, MAM, and SBA were detected in the cytoplasm of the patient fibroblasts (Fig. 4b). As shown in these figures, the lectin-binding profiles differed between lymphocytes and fibroblasts, indicating that the molecules accumulating within the inclusions differ in these two cell types.

HLA-DR expression in lymphocyte subpopulations

To see whether certain molecules expressed on B cells are condensed within the vacuole-like inclusions, HLA-DR expression was compared between the control and patient lymphocytes (Fig. 5). Acetone-fixed CD19⁺ B cells from the patients were stained intensely by FITC-conjugated anti-HLA-DR antibody (Fig. 5Aa). Similarly, extracellular clusters of vacuole-like inclusions were also stained by the antibody (Fig. 5Ab). As compared to B cells, the monocytes from patients expressed only low levels of HLA-DR (Fig. 5Ac). The B cells from normal controls were stained

only vaguely (data not shown). To compare the expression levels of HLA-DR on the cell surface and within the cytoplasm of each cell population, two-color flow cytometry was performed (Fig. 5B, C). In the controls, only CD19⁺ B cells and CD14⁺ monocytes expressed significant levels of HLA-DR on the cell surface (Fig. 5B). The levels of HLA-DR expression did not differ between the cell surface and the cytoplasm, indicating that there is little, if any, contribution of the cytoplasmic fluorescence to the fluorescence intensity of acetone-fixed cells. In patients, HLA-DR expression increased significantly on CD19⁺ B cells after the permeabilization and fixation of the cells (Fig. 5C). This significant increase was only observed in B cells and not in other lymphocyte subpopulations or monocytes.

Expression of class II-related molecules

We further examined the surface and cytoplasmic expressions of various HLA class II molecules, including HLA-DR, HLA-DQ, HLA-DM, and CLIP, all of which are known to be expressed at different stages of endosome maturation and multivesicular antigen processing. Similar levels of HLA-DR, HLA-DQ, and CLIP were expressed on the cell surface and within the cytoplasm in the normal controls (Fig. 6a). HLA-DM was not expressed on the cell surface and was detectable only after permeabilization/fixation, suggesting that it was expressed exclusively within the cytoplasm. In patients with I-cell disease, the profiles of the surface expression of HLA class II molecules were similar to those of the controls. In contrast, the cytoplasmic expression levels of HLA-DR, HLA-DQ,

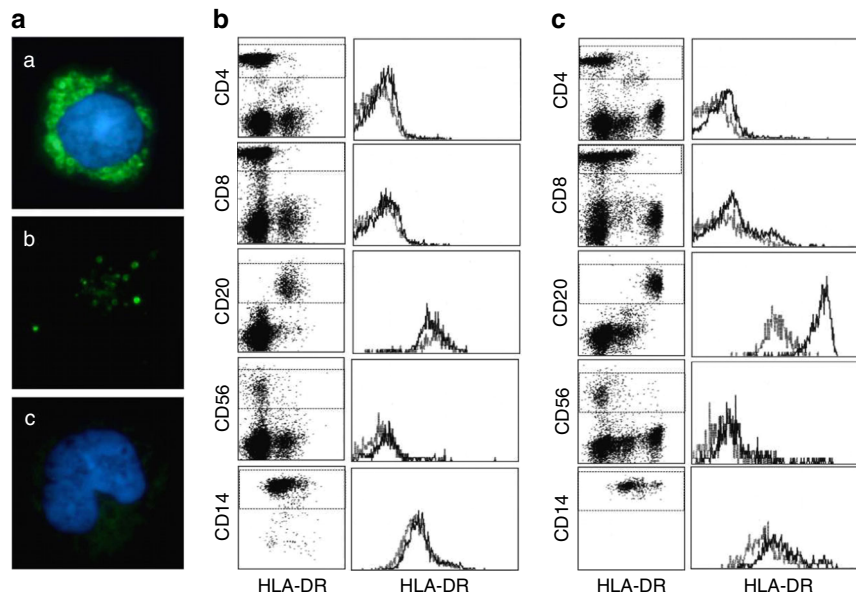


Fig. 5 Expression of HLA-DR. The cytospin preparations of B cells and monocytes from I-cell disease patients were stained with FITC-conjugated anti-HLA-DR antibody. The left columns show the two-color flow cytometry patterns of the cytoplasmic HLA-DR expression. The dotted squares indicate the gating for PE fluorescence analysis for each lymphocyte subpopulation. The right columns show the PE fluorescence profiles of the gated lymphocyte subpopulations. The fine and bold lines indicate the surface and cytoplasmic fluorescence profiles, respectively. The B cells contained a large amount of HLA-DR-positive inclusions (Aa) and the extracellular granules were also HLA-DR-positive (Ab). The monocytes from I-cell disease patients expressed only low levels of HLA-DR (Ac). Flow cytometric analysis of the control (B) and I-cell disease patients (C) revealed intense cytoplasmic HLA-DR expression by B cells (bold lines), whereas the surface HLA-DR expression was much lower (dotted lines)

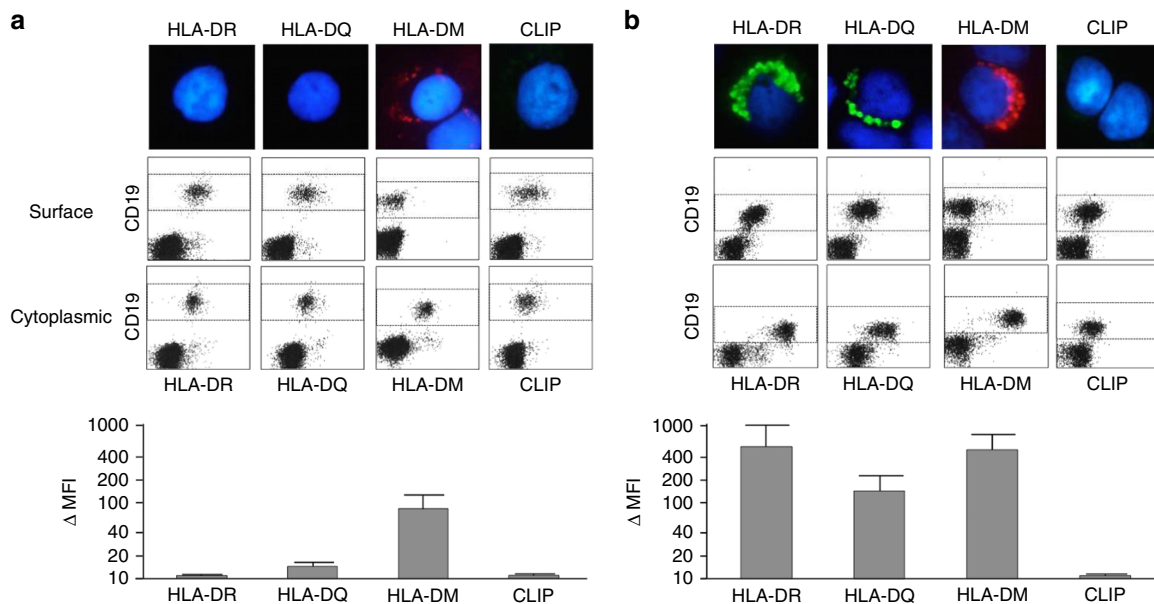


Fig. 6 Expression of HLA class II molecules. B cells were separated from the controls (a) and I-cell disease patients (b) and cytospin preparations were made. Only HLA-DM was detectable within the cytoplasm of the control B cells. In contrast, HLA-DR, HLA-DQ, and HLA-DM were all strongly detected within the cytoplasm of the B cells from I-cell disease patients. Representative staining patterns are shown in the upper row. The flow cytometric profiles of the surface and cytoplasmic expressions of class II-related molecules are shown in the second and third rows, respectively. The fourth row shows the differences in MFI of the cytoplasmic and surface expressions of class II-related molecules. The mean \pm SD of three independent experiments are shown

and HLA-DM were markedly significantly higher than the surface expression levels in the patients. In addition, the CLIP levels did not change (Fig. 6b). In the normal controls, only cytoplasmic HLA-DM expression showed a significant increase (Fig. 6a, lower panel). In the patients with I-cell disease, the Δ MFI of HLA-DR, HLA-DQ, and HLA-DM was significantly increased (Fig. 6b, lower panel).

DISCUSSION

Cytoplasmic vacuole-like inclusions have been reported in various types of cells in I-cell disease.^{10–13} However, the nature of the vacuoles and whether they differ between different cell types is unclear. Although vacuoles are usually observed in all cells of particular tissues or organs in I-cell disease, only a portion of

lymphocytes show vacuole-like inclusions. In contrast to other types of storage disorders, such as Pompe disease or GM1 gangliosidosis, in which the majority of lymphocytes contain vacuoles or non-lymphocytes also contain vacuoles, only a limited fraction of lymphocytes exhibit the vacuole-like inclusions in I-cell disease.^{16–19} In addition, the majority of peripheral blood leukocytes express vacuoles in acute alcoholism.²⁰ These findings suggest that in other types of storage diseases and acute alcoholism, the mechanism of vacuole formation is non-specific. In contrast, it has been strongly suggested that there exists a certain mechanism that can explain the cell lineage-specific accumulation of cytoplasmic vacuole-like inclusions in I-cell disease.

Previous studies have indicated that the impact of GlcNac-1-phosphotransferase enzyme deficiency differs between different types of cells in I-cell disease. For example, the profiles of lysosomal enzymes are distinct between fibroblasts and hepatocytes in I-cell disease, indicating that hepatocytes exhibit a distinct mechanism of lysosomal enzyme transfer that differs from fibroblasts and results in the distinct patterns of vacuole formation in the different cell types.^{21,22} Peripheral blood leukocytes show similar lysosomal enzyme activities in I-cell disease patients and controls.²³ Furthermore, targeting of lysosomal enzymes seems to be independent of M6P in B lymphoblasts from I-cell disease patients.^{24,25} Thus, it is possible that the cytoplasmic inclusions are distinct between fibroblasts and lymphocytes in I-cell disease. To support this, the results of our lectin-binding study clearly showed that the contents of the vacuoles within fibroblasts are distinct from those of lymphocytes, indicating that the mechanism of the accumulation of storage materials within vacuoles differs depending on the cell type.

Because the majority of lymphocytes did not contain the vacuoles, whereas a fraction of lymphocytes contained packed vacuoles within the cytoplasm, we assumed that only a certain subpopulation of lymphocytes contained the vacuoles, although the reason and mechanisms were unknown. Our study with three confirmed cases of I-cell disease showed that only B cells, including virtually all circulating B cells, contained the vacuole-like inclusions. Furthermore, no other cell type, including neutrophils, basophils, eosinophils, monocytes, and lymphocytes, contained the vacuole-like inclusions, suggesting that there is a certain mechanism specific to B cells that enables the accumulation of vacuole-like inclusions in the cells.

The accumulation of MHC class II-containing compartment (MIIC) structures has been reported in B cells and B-cell lines in I-cell disease patients.²⁶ Although there has been no study connecting the vacuole-like inclusions with the accumulation of MIIC structures, our study strongly indicates that the characteristic vacuole-like inclusions in the B cells of I-cell disease patients reflect the accumulation of MIIC structures. The intense cytoplasmic staining of the HLA class II molecules in the B cells from I-cell disease patients further supports the hypothesis that GlcNac-1-phosphotransferase deficiency leads to the abnormal transport of HLA class II molecules in the B cells, resulting in the characteristic pattern of vacuole-like inclusions observed exclusively in the B cells in I-cell disease.

Further studies are needed to elucidate the reason why only B cells showed the vacuole-like inclusions and how HLA class II molecules accumulate within the vacuole-like inclusions or MIIC structures. The comparison of lysosomal enzyme activity among different lymphocyte subpopulations may clarify the distinct roles of the enzyme in different cell types. In addition, *in vitro* studies using induced pluripotent stem cells from patients with corrected enzyme activity may directly show the importance of the enzyme activity for the characteristic morphology of B cells.

The very fact that virtually all circulating B cells, and only B cells, expressed vacuole-like inclusions in I-cell disease offers a novel and sensitive diagnostic aid for the early and prompt diagnosis of

I-cell disease in infants with suspected clinical features. Furthermore, the accumulation of HLA class II molecules in B cells may have yet unknown immunological impacts and may affect the immune functions in these patients. In this respect, Otomo et al. recently reported in a mouse model that mannose-6 phosphorylation of lysosomal enzymes controls B-cell functions and results in impaired antibody production in I-cell disease.²⁷ The impact of the B-cell dysfunction may appear later in life, but because of the short life expectancy of these patients, we may not be able to observe the long-term consequences.

A limitation of the current study is that we could not perform similar examinations for patients with other types of storage diseases, including Pompe disease and GM1 gangliosidosis. Future studies are expected to reveal whether different mechanisms of vacuole formation exist in different types of storage diseases.

ACKNOWLEDGEMENTS

We would like to thank Ms. Harumi Matsukawa for her excellent technical assistance. This work was supported by a Grant-in-Aid for Scientific Research from the Ministry of Education, Culture, Sports, Science, and Technology of Japan, and a grant from the Ministry of Health, Labour, and Welfare of Japan, Tokyo.

AUTHOR CONTRIBUTIONS

A.Y. and Y.I.-H.: Provided substantial contributions to the conception and design of the study, the acquisition of data, and the analysis and interpretation of the data. T.T.: Provided critical advice for the technical aspects of the study. M.K.: Drafted the article and revised it critically for important intellectual content. Y.N. and A.Y.: Provided final approval of the version to be published.

ADDITIONAL INFORMATION

Competing interests: The authors declare no competing interests.

Publisher's note: Springer Nature remains neutral with regard to jurisdictional claims in published maps and institutional affiliations.

REFERENCES

1. Leroy, J. G. & DeMars, R. I. Mutant enzymatic and cytological phenotypes in cultured human fibroblasts. *Science* **157**, 804–806 (1967).
2. Leroy, J. G. et al. I-cell disease: a clinical picture. *J. Pediatr.* **79**, 360–365 (1971).
3. Patriquin, H. B. et al. Neonatal mucopolidosis II (I-cell disease): clinical and radiologic features in three cases. *Am. J. Roentogenol.* **129**, 37–43 (1977).
4. Okada, S. et al. I-cell disease: clinical studies of 21 Japanese cases. *Clin. Genet.* **28**, 207–215 (1985).
5. Tiede, S. et al. Mucopolidosis II is caused by mutations in GNPTA encoding the α/β GlcNac-1-phosphotransferase. *Nat. Med.* **11**, 1109–1112 (2005).
6. Kudo, M., Brem, M. S. & Canfield, W. M. Mucopolidosis II (I-cell disease) and mucopolidosis IIIA (classical pseudo-Hurler polydystrophy) are caused by mutations in the GlcNac-1-phosphotransferase α/β -subunits precursor gene. *Am. J. Hum. Genet.* **78**, 451–463 (2006).
7. Tiede, S. et al. Missense mutation in the N-acetylglucosamine-1-phosphotransferase gene (GNPTA) in a patient with mucopolidosis II induces changes in the size and cellular distribution of GNPTG. *Hum. Mutat.* **27**, 830–831 (2006).
8. Brulke, T., Pohl, S. & Storch, S. Molecular analysis of the GlcNac-1-phosphotransferase. *J. Inher. Metab. Dis.* **31**, 253–257 (2008).
9. Reitman, A. L., Verki, A. & Kornfield, S. Fibroblasts from patients with I-cell disease and pseudo-Hurler polydystrophy are deficient in uridine 5-diphosphate-N-acetylglucosamine: glycoprotein N-acetylglucosaminylphosphotransferase activity. *J. Clin. Invest.* **67**, 1574–1579 (1981).
10. Koga, M. et al. Histochemical and ultrastructural studies of inclusion bodies found in tissues from three siblings with I-cell disease. *Pathol. Int.* **44**, 223–229 (1994).
11. Tang, X. et al. I-cell disease: report of an autopsy case. *Tokai J. Exp. Clin. Med.* **20**, 109–120 (1995).
12. Carey, W. F. et al. Prenatal diagnosis of mucopolidosis II—electron microscopy and biochemical evaluation. *Prenat. Diag.* **19**, 252–256 (1999).
13. Van der Meer, W. et al. Peripheral blood lymphocyte appearance in a case of I cell disease. *J. Clin. Pathol.* **54**, 724–726 (2001).

14. Kawashima, I. et al. Cytochemical analysis of storage materials in cultured skin fibroblasts from patients with I-cell disease. *Clin. Chim. Acta* **378**, 142–146 (2007).
15. Toga, A. et al. Clinical significance of cloned expansion and CD5 down-regulation in Epstein-Barr virus (EBV)-infected CD8⁺ T lymphocytes in EBV-associated hemophagocytic lymphohistiocytosis. *J. Infect. Dis.* **201**, 1923–1932 (2010).
16. Lynch, D. T. & Czuchlewski, D. R. Peripheral blood findings in GM1 gangliosidosis. *Blood* **127**, 2161 (2016).
17. Smith, H. & Collins, R. J. A population of lymphocytes in human blood distinctive in morphology and other characteristics. *J. Clin. Pathol.* **30**, 243–249 (1977).
18. Hagemans, M. L. C. et al. PAS-positive lymphocyte vacuoles can be used as diagnostic screening test for Pompe disease. *J. Inherit. Metab. Dis.* **33**, 133–139 (2010).
19. Anderson, G. et al. Blood film examination for vacuolated lymphocytes in the diagnosis of metabolic disorders; retrospective experience of more than 2500 cases from a single centre. *J. Clin. Pathol.* **58**, 1305–1310 (2005).
20. Davidson, R. J. & McPhie, J. L. Cytoplasmic vacuolation of peripheral blood cells in acute alcoholism. *J. Clin. Pathol.* **33**, 1193–1196 (1980).
21. Dittmer, F. et al. Alternative mechanisms for trafficking of lysosomal enzymes in mannose 6-phosphate receptor-deficient mice are cell type-specific. *J. Cell Sci.* **112**, 1591–1597 (1999).
22. Griffiths, G. M. & Isaacs, S. Granzymes A and B are targeted to the lytic granules of lymphocytes by the mannose-6-phosphate receptor. *J. Cell Biol.* **120**, 885–896 (1993).
23. Kato, E., Yokoi, T. & Taniguchi, N. Lysosomal acid hydrolases in lymphocytes of I-cell disease. *Clin. Chim. Acta* **95**, 285–290 (1979).
24. Tsuji, A., Omura, K. & Suzuki, Y. I-cell disease: evidence for a mannose 6-phosphate independent pathway for translocation of lysosomal enzymes in lymphoblastoid cells. *Clin. Chim. Acta* **176**, 115–121 (1988).
25. Glickman, J. N. & Kornfeld, S. Mannose 6-phosphate-independent targeting of lysosomal enzymes in I-cell disease B lymphoblasts. *J. Cell Biol.* **123**, 99–108 (1993).
26. Glickman, J. N. et al. The biogenesis of the MHC class II compartment in human I-cell disease B lymphoblasts. *J. Cell Biol.* **132**, 769–785 (1996).
27. Otomo, T. et al. Mannose 6 phosphorylation of lysosomal enzymes controls B cell functions. *J. Cell Biol.* **208**, 171–180 (2015).